CTFF3 TECHNICAL NOTE

INFN - LNF, Accelerator Division

Frascati, March 6, 2002

Note: **CTFF3-006**

NEW DESIGN FOR THE DELAY LOOP IN CTF3

C. Biscari

1. INTRODUCTION

The delay loop (DL), in the frequency multiplication scheme of CTF3, doubles the peak current of the drive beam. The preservation of the transverse and longitudinal beam structures asks for isochronicity, path length tuning, and large energy acceptance in the device.

A first preliminary design of the ring was already presented [1], in which each one of the four arcs of the ring was achromatic and nearly isochronous, with the full isochronocity condition fulfilled in each half of the ring. The isochronicity corresponds to strong horizontal focusing, which of course makes the ring structure critical against tolerances.

A different design is here presented, which corresponds to achromaticity and isochronicity fulfilled in each half of the ring. This more relaxed condition, still assuring the preservation of the longitudinal phase plane, is less critical from the point of view of transverse beam dynamics. The total number of quadrupoles and their fields are strongly reduced. The ring layout, dipole, injection / extraction position, matching with the transfer lines, are the same of the previous design.

Table 1 shows a summary of the main DL parameters and requirements. The energy range of CTF3 is slightly changed [2] with respect to the previous design: it has been reduced to 150-300 MeV, corresponding to the high-low current regime respectively.

Table I - Delay Loop and beam parameters

Length [m]	42
Energy [MeV]	150-300
Emittance [μrad] (ε_n = 100 μrad)	0.34-0.17
Bunch length (rms) [mm]	0.5
Charge/Bunch [nC]	2.3-0.5
Isochronicity	$\lvert R_{56}\rvert$ < 0.02m
Momentum Acceptance (total)	$\Delta p/p = 5\%$
Path Length Tuning [mm]	±0.5

2. DELAY LOOP DESCRIPTION

The great part of the DL magnetic components are copies of already existing magnets, as it was pointed out in [1] and according to the CTF3 philosophy of reusing when possible existing hardware, design material and documentation. The reduction of both the quadrupole number and of their strengths could probably fit the reutilization of some of the existing EPA quadrupoles, but in this design all quadrupoles are of the same type of DAFNE Accumulator ones [3], as they were in the previous design. Sextupoles are also based on the DAFNE Accumulator design [4], and so are the two different septa [5], with the only difference that the larger one, bending by 27.14°, is shorter than the original DAFNE design. The ten dipoles are equal to the EPA ones [6], but used at a different radius of curvature. Figure 2 shows the DL layout, while the main parameters of the magnetic elements are listed in Table II.

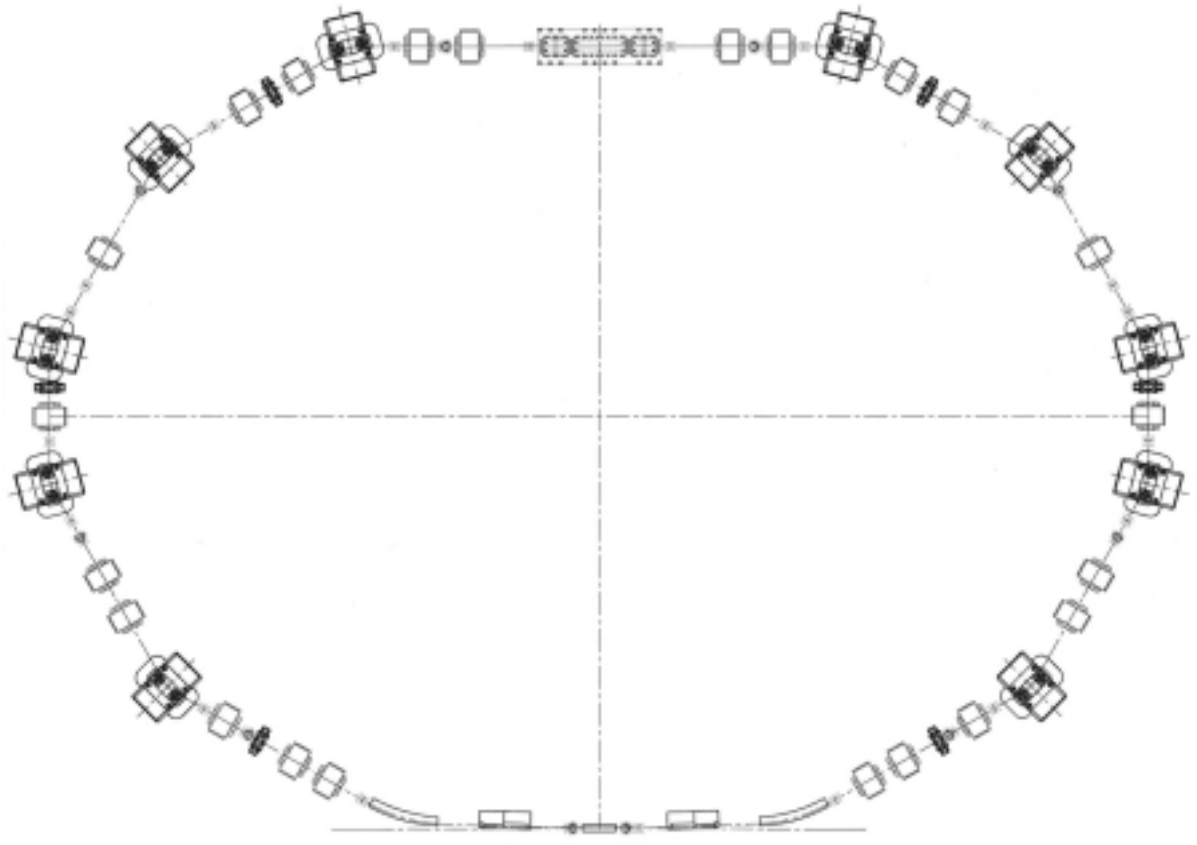

Figure 1. Delay Loop Layout.

Table II - Delay Loop Magnetic Elements.

A)	Number of Dipoles (EPA-like)	10
	Dipole Bending Radius [m]	1.079
	Dipole Bending Angle [°]	30
	Dipole Field [T] (150/300 MeV)	0.50/1.00
	Integrated Quadrupole Coeff. in Dipoles [T] (150/300 MeV)	0.15/0.30
B)	Number of Quadrupoles (DAΦNE Accumulator-like)	22
	Magnetic length [m]	0.3
	Max. Integrated Gradient [T] (150/300 MeV)	0.8/1.6
	Quadrupole Families	11
C)	Number of Sextupoles (DAΦNE Accumulator-like)	6
	Magnetic length [m]	0.1
	Max Integrated Gradient [T/m] (150/300 MeV)	3/6
	Sextupole Families	3
D)	Number of Path Length Tuning Wiggler	1
E)	Number of 2° Septa (DAΦNE Accumulator-like)	2
F)	Number of 27°.14 Septa (DAΦNE Accumulator-like)	2
G)	Injection Dipoles Number	2
	Injection Dipoles Bending Angle [mrad]	5

3. *LINEAR LATTICE*

The first order isochronicity condition, corresponding to independence of the particle path length on its energy, is written usually as

$$R_{56} = -\int \frac{D_x}{\rho} ds = 0 \qquad (1)$$

where **R** is the first order 6x6 transport matrix, D_x is the dispersion function and ρ is the curvature radius in the dipoles. Storage rings have usually negative values of R_{56}, which means that particles with higher energies travel along longer paths. The isochronicity condition requires strong horizontal focusing to force the dispersion to negative values in some of the dipoles.

The DL can be divided into four parts. It has been already pointed out in the introduction how critical is the solution in which each arc of the loop is nearly isochronous. In the present design both the achromaticity and the isochronicity are fulfilled in each half ring. This condition implies a more relaxed horizontal focusing and lower chromaticity. Furthermore the total number of quadrupoles is reduced. The half ring achromaticity assures the dispersion free section where the path length tuning wiggler is housed.

The DL lattice is symmetric around the center of the wiggler. Figure 2 shows the optical functions, calculated with MAD8. The figure includes the input and output sections, 3.6 m long, with the small dipoles, which take the beam to and from the RF deflector.

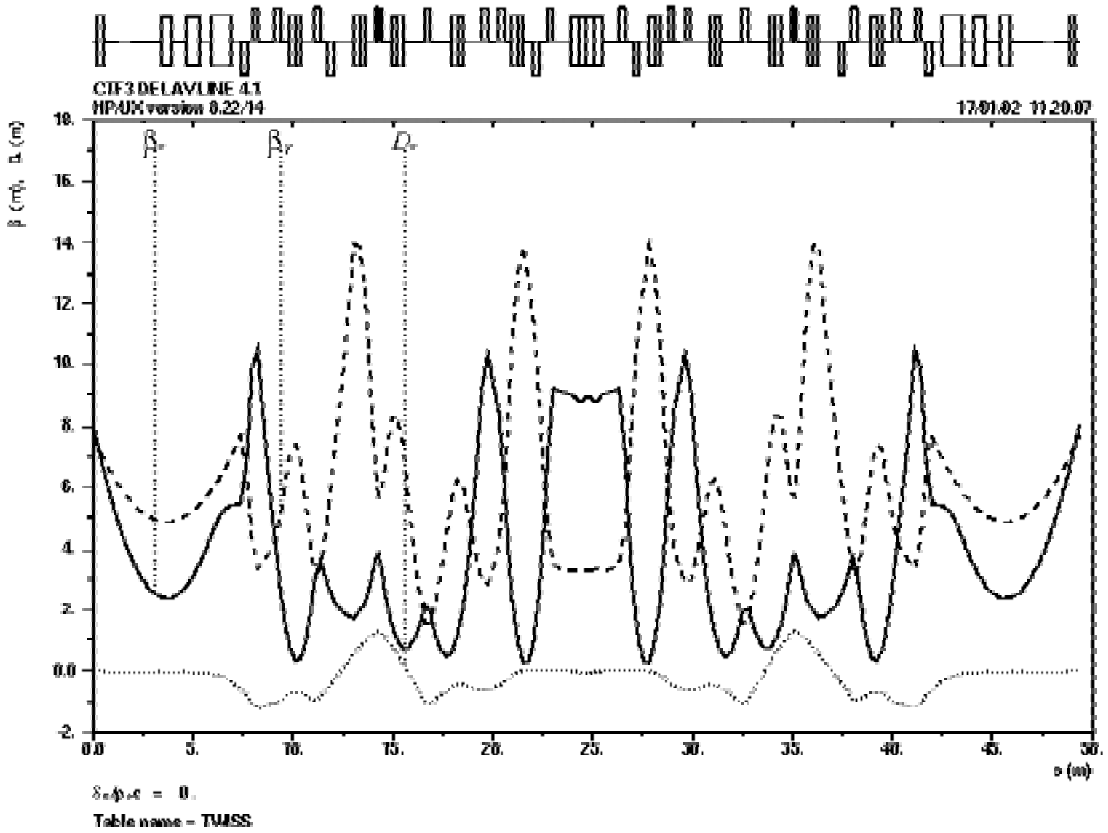

Figure 2. Delay Loop Optical Functions.

Table III - Delay Loop Main Optical Parameters.

Max. Horizontal Beta [m]	10.5
Max. Vertical Beta [m]	14.0
Max. Dispersion [m]	1.3
Horizontal Betatron Phase Advance	3.96
Vertical Betatron Phase Advance	1.38
Horizontal natural chromaticity	-6
Vertical natural chromaticity	-8

The RF deflector position corresponds in the figure to the first and last betatron function waists, whose relative distance is the DL length, 42 m. In Table III the main optical parameters are listed; the phase advances refer to the 42 m long DL. The design is flexible enough to change the phase advance of the whole loop within some tenths of degrees. The quadrupole strengths are listed in the Appendix. The model used for the bends is the one by T. Risselada (January 2001) based on magnetic measurements [7].

Tuning of the R_{56} term, in the range of few cm, is achieved by changing the strengths of three quadrupole families, mantaining the zero dispersion in the wiggler section, and affecting negligibly the overall betatron functions. Figure 3 shows the amount of the almost linear variation of the three quadrupoles to change the R_{56} term in the requested range. Larger variations can be done of course using all the quadrupole families.

The line seen by the even bunches, as explained in [1], is matched with the odd bunches, if the two transverse betatron waists coincide at the symmetry point. The values of the betatron function in this point are β_{wx} = 2.4 m and β_{wy} = 4.9 m.

The path length can be varied with the wiggler by ±4 mm[8], well above the original requirements [1].

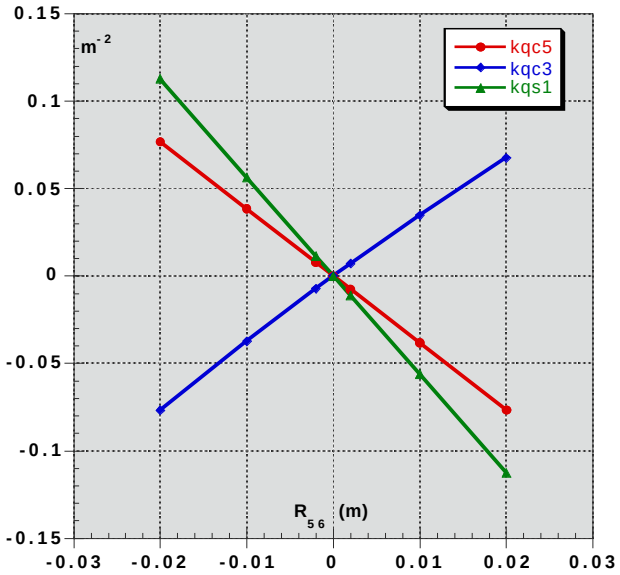

Figure 3 – Change in the three quadrupole families which tune the R_{56} term by few cm.

4. *SECOND ORDER BEAM DYNAMICS*

In the following all considerations refer to single-particle dynamics, i.e. no collective effects will be considered. The conservation of both transverse and longitudinal emittances in the DL must be considered together, since the strong sextupolar correction needed for 2nd order isochronicity is in general dangerous for the transverse plane preservation.

The first order isochronicity condition does not assure the longitudinal emittance preservation, even for particles with no transverse invariant. The dependence of the longitudinal position on the energy deviation is correlated also to the transverse particle coordinates:[1]:

$$ct = (ct)_{0+} R_{56} \frac{\Delta p}{p} + T_{516}\, x_0 \frac{\Delta p}{p} + T_{526}\, x'_0 \frac{\Delta p}{p} + T_{536}\, y_0 \frac{\Delta p}{p} + \\ + T_{546}\, y'_0 \frac{\Delta p}{p} + T_{556}\, (ct)_0 \frac{\Delta p}{p} + T_{566} \left(\frac{\Delta p}{p}\right)^2 \qquad (3)$$

where T_{ijk} are the elements of the second order transfer matrix **T** [9]. Isochronicity is achieved when:

$$T_{5i6} = 0 \qquad \forall\, i \qquad (4)$$

In a line with no vertical bendings the terms relating *ct* with the vertical phase plane, T_{536} and T_{546}, are zero. T_{556} is zero, when only magnetic elements are present in the line, since they do not affect the energy of the particles.

The condition (4) can be satisfied therefore with three sextupoles, but the non-linearities of such sextupoles produce transverse emittance filamentation. In fact they modify the other terms of **T**, both those relating the transverse planes to the energy spread (T_{ij6}, for $i, j = 1, 2, 3, 4$) and those purely transverse (T_{ijk}, for $i, j, k = 1, 2, 3, 4$).

Six-dimensional tracking, using the MAD8 code, has been performed and a sextupole configuration has been found which preserves the three phase plane emittances within the nominal values. A large number of particles (1000), with gaussian-distributed coordinates in the 6 planes *(x, p_x, y, p_y, ct, Δp/p)* has been tracked in different situations. The tracking has been performed starting from the small dipole before the DL (initial point in Fig. 2) up to its symmetric position (final point in Fig. 2). The initial beam parameters correspond to the more critical situation: low energy (150 MeV), large emittance and large energy spread, as listed in Table IV.

Table IV – Beam parameters used in simulations

ε_x (μrad)	0.4
ε_y (μrad)	0.4
Δp/p (rms)	0.008
σ_l (mm) (rms)	0.5

In Table V the beam parameters obtained from the tracking are listed. To be noticed that the rms values of the input particle distribution correspond to ~ 93% of the original rms (see table IV). This is due to the ~ 2.5σ truncation of the one-dimensional gaussian [10]. The emittance, obtained as rms value from the particle coordinate distributions,

$$\varepsilon_w = \sqrt{\langle w^2 \rangle \langle p_w^2 \rangle - \langle w p_w \rangle^2} \quad w = x, y \tag{5}$$

corresponds to ~ 85% of the original value, due to the truncation of a two-dimensional gaussian.

Table V – Beam parameters obtained from simulations

	Input	output A – no sext	output B – $T_{566} = 0$	output C – 3 sext
ε_x (μrad)	0.34	0.48	2.33	0.47
β_x (m)	8.1	7.4	6.1	7.5
α_x	1.5	- 1.7	- 1.5	-1.2
ε_y (μrad)	0.34	0.35	0.41	0.37
β_y (m)	7.7	8.2	11.0	8.8
α_y	0.7	- 0.8	- 0.8	- 0.8
Δp/p (rms)	0.0074	0.0074	0.0074	0.0074
σ_l (mm) (rms)	0.46	1.79	0.97	0.55

For a $R_{56} = 0$ lattice with no sextupoles, the dominant term in expression (3) is the one relating the position in the bunch with the energy deviation, T_{566}. Let's remind that even in absence of sextupoles the 2nd order matrix terms are not zero [9]. Figure 4 shows the three phase planes of the bunch distribution at the input of the DL (initial point of Fig. 2), and the corresponding output, at the symmetric position. While the two transverse planes are slightly affected by the passage in the DL, the longitudinal phase plane shows the 2nd order correlation between the energy deviation and the position in the bunch ($T_{566} = -18.4$ *m*).

Correcting only this term in each half ring by using one sextupole family, a strong horizontal emittance degradation appears (see Fig. 4 and Table V). The terms relating the horizontal coordinates to the energy deviation increase by a large amount, especially T_{126} (see Table A3 in the Appendix). The case (not reported here) in which three sextupoles are used to correct also the T_{516} and T_{526} terms produces an even larger transverse emittance degradation.

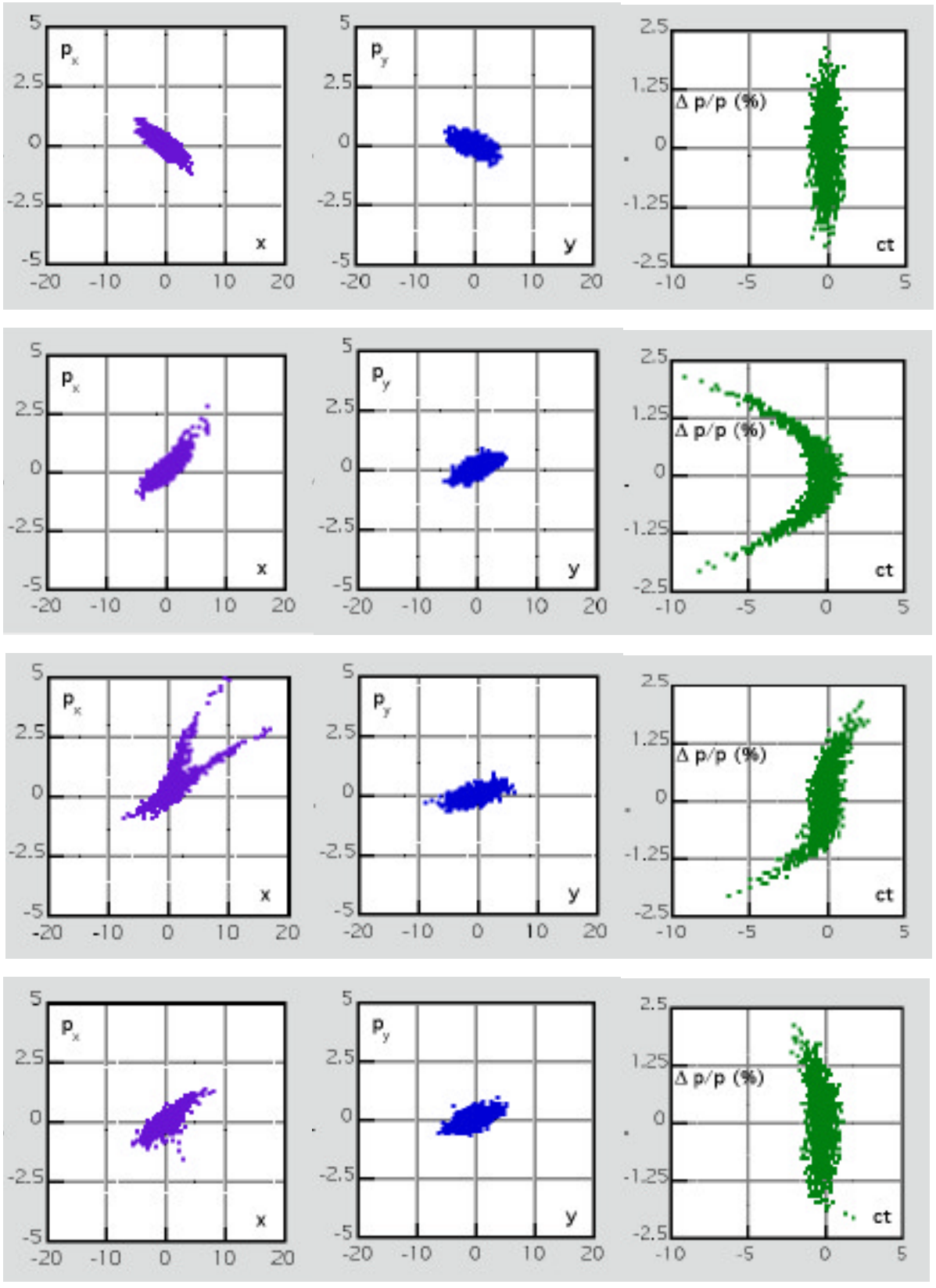

Figure 4. Horizontal, Vertical and Longitudinal Phase Spaces at : O) DL Input; A) DL Output – no sextupoles; B) DL Output – T_{566} = 0; C) DL Output – 3 sextupole families. Dimensions are in mm, and momenta in mrad.

Distributing in three sextupole families the correction, the change in the T_{ij6} (i,j = 1,2) terms is minimized and a good compromise between longitudinal and transverse emittance preservation is found, with a value for T_{566} = – 3.6 m. The emittance growth does not depend on the bunch length (T_{ij5} = 0, i, j = 1, .., 4), while it does strongly on the energy spread. Figure 5 shows the ratio between the initial and the final emittance of the distribution in the horizontal and in the vertical plane for the three cases above considered. The value of the emittance, computed with expression (5), in the cases in which the gaussian shape is lost, is dominated by the tails of the distribution. The tracking has been done using the transverse emittances and the bunch length of table IV, and changing the rms energy spread of the distribution. The lattice is more critical in the horizontal than in the vertical plane, due to the isochronicity condition. The solution C) produces negligible emittance growth up to values of 0.008 rms energy spread, which correspond to the requested ± 2.5% energy acceptance of the loop. Figure 6 shows the relative rms bunch length; in the case of no sextupoles (A) the length obviously increases quadratically. The best solution is again the one with the distributed sextupole correction.

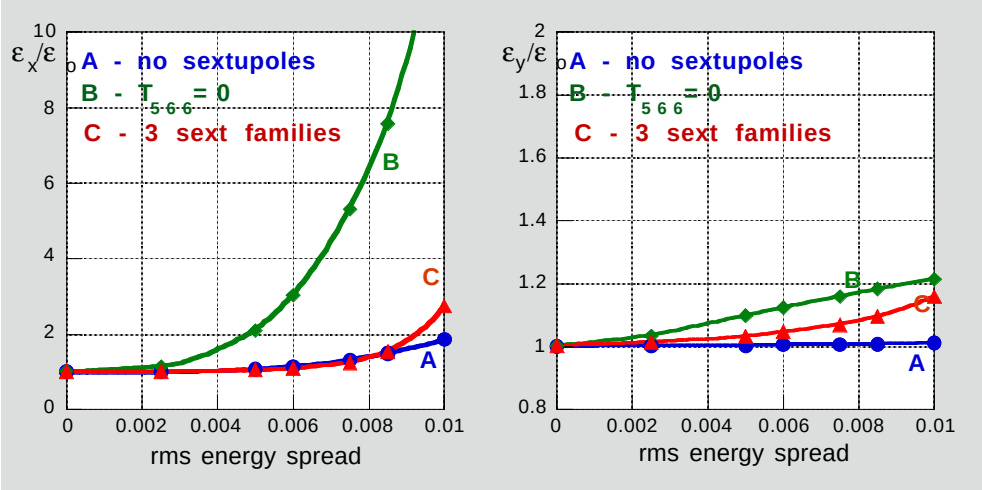

Figure 5 – Ratio between final and initial emittances (horizontal and vertical) as a function of the rms energy spread of the longitudinal gaussian distribution in the case of no sextupoles (A), one sextupole family correcting the T_{566} term (B) and three sextupole families (C).

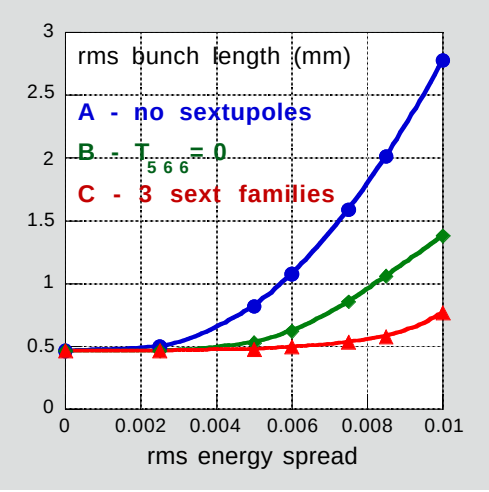

Figure 6 – Rms bunch length as a function of the rms energy spread of the longitudinal gaussian distribution for the same three cases.

The emittance degradation dependence on the initial value of the emittance has been also investigated. Tracking done with the nominal longitudinal phase plane parameters (Table IV), and with different initial emittances, ε_{xo}, has shown that in the case of optimized sextupole configuration (C) the increase of emittance is almost constant for any value of ε_{xo}. The relative degradation is therefore higher for smaller emittances (see Fig. 7), and this is in general true for all the studied configurations.

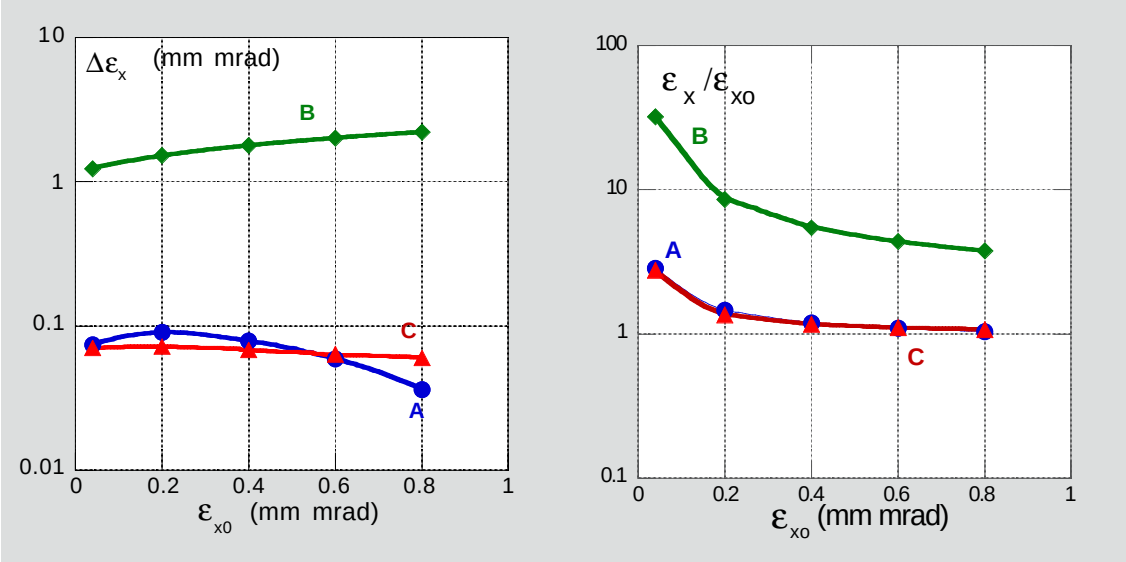

Figure 7 – Horizontal emittance increase and final to initial emittance ratio as a function of the initial emittance for the three cases considered.

5. *BEAM STAY CLEAR REQUIREMENTS*

The criteria of defining the vacuum chamber acceptance greater than ten times the rms betatron beam envelope plus 5% energy acceptance will be used. Figures 8 and 9 show the rms beam envelopes along the DL in the horizontal and vertical plane respectively.

Envelopes have been calculated according to:

$$\sigma_w = \sqrt{\beta_w \varepsilon_w} + \left| D_w \Delta p / p \right| \qquad w = x, y \tag{5}$$

with $\varepsilon_x = \varepsilon_y = 0.4\,mm\,mrad$ and $\Delta p/p = 0.833\,\%$.

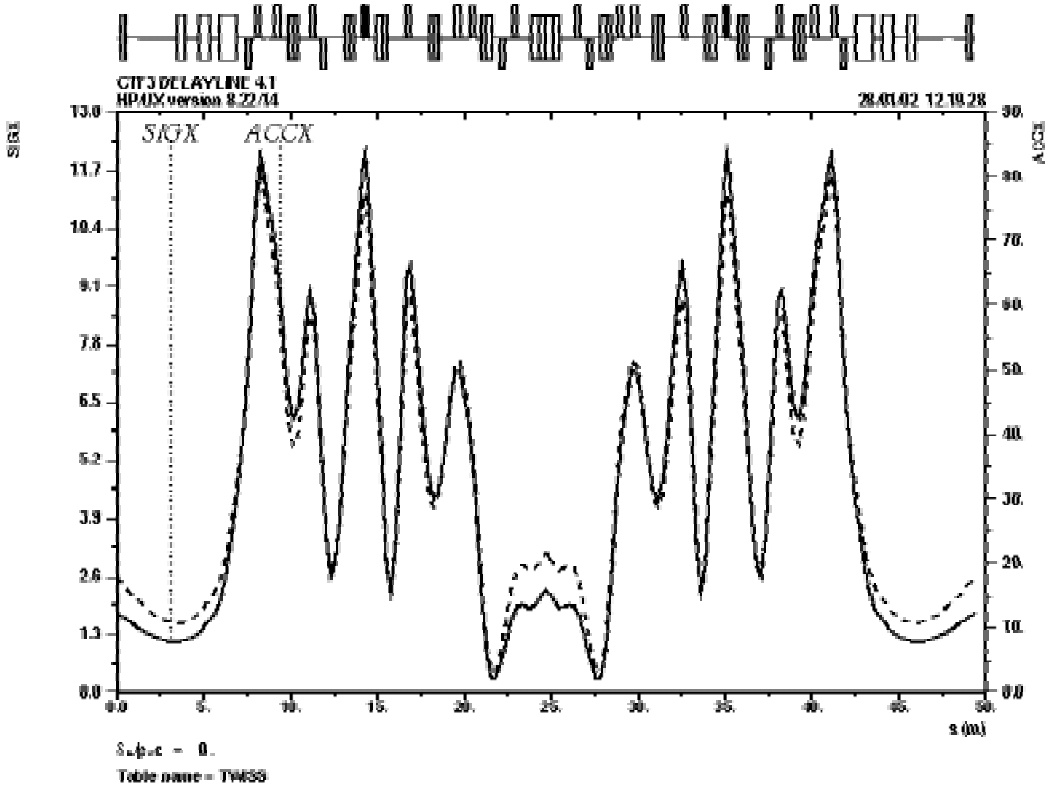

Figure 8. DL Beam Horizontal Envelopes (full line, left axis - rms values) and Total Beam Stay Clear (dashed line, right axis) in mm

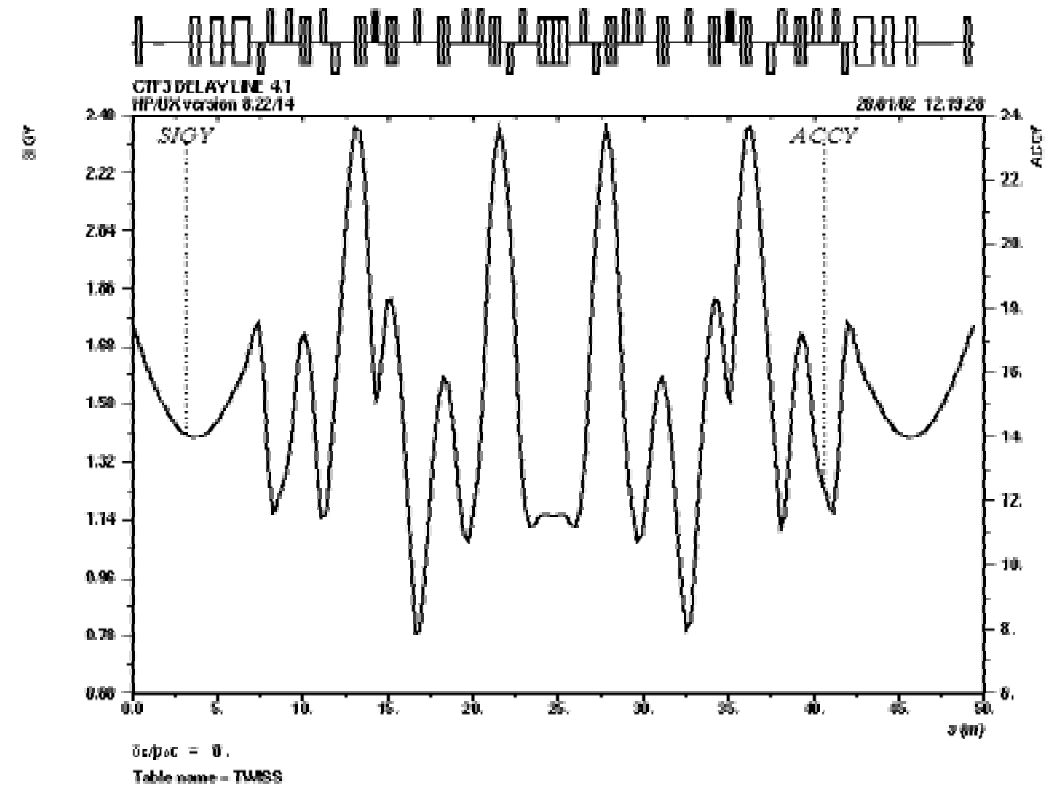

Figure 8. DL Beam Vertical Envelopes (left axis, rms values) and Total Beam Stay Clear (right axis) in mm. The two lines obviously coincide.

The total vacuum chamber apertures must be at least 80 mm and 25 mm in the horizontal and vertical planes respectively, considering that trajectory allowances are already included in the ten-sigma acceptance.

Table VI shows the gaps of the DL elements. In the case of the Injection Dipoles and of the RF Deflector, the only elements not yet designed, the gaps are suggested.

Table VI - Delay Loop Elements Gaps.

Element	Horizontal [mm] (total)	Vertical [mm] (total)
Dipoles	136	42
Quadrupoles	100 (Ø)	100 (Ø)
Sextupoles	100 (Ø)	100 (Ø)
Wiggler	100	40
2° Septa	20 (Ø)	20 (Ø)
27.14° Septa *	> 35	> 20
Injection Dipoles *	> 30	> 30
RF Deflector *	> 30	> 30

* Suggested

All the element apertures fit the acceptance requirements, except the 27.14° septum in the horizontal plane, since its vacuum chamber has a diameter of 20 mm. The design of a new vacuum chamber for this element, with a horizontal total aperture of at least 35 mm, is therefore required, together with the corresponding magnet modifications.

6. CONCLUSIONS

The main challenge from the point of view of the beam dynamics in the CTF3 multiplication system is the manipulation of very short bunches at high current and high charge. The requirements on emittance preservation pose serious constraints on the optics design. Smooth linear optics and adequate sextupole compensation can ensure the isochronicity up to the second order. The influence of collective effects (wake fields and coherent synchrotron radiation) is not treated in this note.

REFERENCES

[1] F.Sannibale, Driving Beam Delay Loop Design for CTF3, Technical Note CTFF3 – 001, April 2001.

[2] CTF3 review, October 2001, CERN.

[3] B. Bolli et al., Measurements on Tesla Quadrupole Prototype for the DAFNE Accumulator and Main Rings, DAFNE Technical Note MM-4, December 2, 1994.

[4] B. Bolli et al., The DAFNE Accumulator Sextupoles, DAFNE Technical Note MM-6, May 10, 1995.

[5] B. Bolli et al., The Injection/extraction 2 deg Septum Magnets of the DAFNE Accumulator, DAFNE Technical Note MM-7, June 7, 1995.

[6] LEP Preinjector Parameter List (EPA part), PS/LPI Note 88-02, March 1988 (rev.).

[7] R. Chritin and D. Cornuet, SL-Note-2000-031 MS (2000).

[8] C.Biscari, Combiner Ring Lattice, CTFF3 – 002, April 2001.

[9] F.C.Iselin, The MAD Program, version 8.13, Physical Methods Manual, CERN/SL/92 – (AP).

[10] B.Bru and M.Weiss, Design of the low energy beam transport system for the new 50 MeV Linac, CERN/MPS/LIN 74 –1.

APPENDIX

Table A1 - Quadrupole Families Strengths.

Family Name	k^2 [m^{-2}]
Qs1	-2.61
Qs2	3.43
Qs3	0.93
Qc1	4.37
Qc2	-0.29
Qc3	3.73
Qc4	5.27
Qc5	2.43
Qc6	2.29
Qw1	-1.39
Qw2	3.06

Table A2 - Sextupole Families Strengths.

Family Name	Sext./Family	L [m]	k [m^{-3}]
Sf1	2	0.1	- 55
Sf2	2	0.1	50
Sf3	2	0.1	-45

Table A3 – Terms of the 2nd order transport matrices

	A)	B)	C)
T111	0.7	-9.8	8.9
T112 = T121	-1.2	-87.3	-23.0
T122	0.4	29.4	27.1
T133	0.1	7.1	-6.7
T134 = T143	0.2	37.2	-24.5
T144	3.8	-131.1	-10.3
T116	-4.9	9.1	6.4
T126	-30.0	203.6	94.5
T166	-1.7	-1.1	3.3
T211	-2.5	-1.8	-35.1
T212 = T221	0.8	0.6	12.5
T222	0.7	90.4	17.7
T233	-0.3	-0.6	4.4
T234 = T243	-0.4	-4.3	-6.4
T244	-11.5	-101.2	70.7
T216	9.0	7.3	-2.7
T226	-4.9	10.2	6.7
T266	3.8	10.7	1.1
T516	-3.8	-10.6	-0.8
T526	1.3	3.6	2.8
T566	-18.4	0.0	-3.6